

STUDY OF DECAY MECHANISMS IN $B^- \rightarrow \Lambda_c^+ \bar{p} \pi^-$ DECAY AND OBSERVATION OF LOW MASS STRUCTURE IN THE $(\Lambda_c^+ \bar{p})$ SYSTEM

N. Gabyshev,¹ K. Abe,⁸ K. Abe,⁴⁰ I. Adachi,⁸ H. Aihara,⁴² Y. Asano,⁴⁶ V. Aulchenko,¹ T. Aushev,¹² A. M. Bakich,³⁷ U. Bitenc,¹³ I. Bizjak,¹³ S. Blyth,²⁵ A. Bondar,¹ A. Bozek,²⁶ M. Bračko,^{8,19,13} J. Brodzicka,²⁶ T. E. Browder,⁷ P. Chang,²⁵ Y. Chao,²⁵ A. Chen,²³ W. T. Chen,²³ B. G. Cheon,³ R. Chistov,¹² S.-K. Choi,⁶ Y. Choi,³⁶ A. Chuvikov,³³ S. Cole,³⁷ J. Dalseno,²⁰ M. Danilov,¹² M. Dash,⁴⁷ A. Drutskoy,⁴ S. Eidelman,¹ Y. Enari,²¹ S. Fratina,¹³ T. Gershon,⁸ G. Gokhroo,³⁸ B. Golob,^{18,13} A. Gorišek,¹³ T. Hara,³⁰ H. Hayashii,²² M. Hazumi,⁸ T. Hokuue,²¹ Y. Hoshi,⁴⁰ S. Hou,²³ W.-S. Hou,²⁵ Y. B. Hsiung,²⁵ T. Iijima,²¹ A. Imoto,²² K. Inami,²¹ A. Ishikawa,⁸ R. Itoh,⁸ M. Iwasaki,⁴² Y. Iwasaki,⁸ J. H. Kang,⁴⁸ J. S. Kang,¹⁵ S. U. Kataoka,²² N. Katayama,⁸ H. Kawai,² T. Kawasaki,²⁸ H. R. Khan,⁴³ H. Kichimi,⁸ H. J. Kim,¹⁶ H. O. Kim,³⁶ S. K. Kim,³⁵ S. M. Kim,³⁶ K. Kinoshita,⁴ S. Korpar,^{19,13} P. Krokovny,¹ S. Kumar,³¹ C. C. Kuo,²³ A. Kuzmin,¹ Y.-J. Kwon,⁴⁸ J. S. Lange,⁵ G. Leder,¹¹ T. Lesiak,²⁶ S.-W. Lin,²⁵ F. Mandl,¹¹ T. Matsumoto,⁴⁴ Y. Mikami,⁴¹ W. Mitaroff,¹¹ H. Miyake,³⁰ H. Miyata,²⁸ R. Mizuk,¹² T. Nagamine,⁴¹ Y. Nagasaka,⁹ E. Nakano,²⁹ M. Nakao,⁸ H. Nakazawa,⁸ Z. Natkaniec,²⁶ S. Nishida,⁸ O. Nitoh,⁴⁵ S. Ogawa,³⁹ T. Ohshima,²¹ T. Okabe,²¹ S. Okuno,¹⁴ S. L. Olsen,⁷ Y. Onuki,²⁸ H. Ozaki,⁸ H. Palka,²⁶ C. W. Park,³⁶ H. Park,¹⁶ N. Parslow,³⁷ L. S. Peak,³⁷ R. Pestotnik,¹³ L. E. Piiilonen,⁴⁷ M. Rozanska,²⁶ H. Sagawa,⁸ Y. Sakai,⁸ N. Sato,²¹ T. Schietinger,¹⁷ O. Schneider,¹⁷ A. J. Schwartz,⁴ K. Senyo,²¹ R. Seuster,⁷ M. E. Sevier,²⁰ H. Shibuya,³⁹ V. Sidorov,¹ J. B. Singh,³¹ A. Somov,⁴ R. Stamen,⁸ S. Stanič,^{46,*} M. Starič,¹³ T. Sumiyoshi,⁴⁴ S. Y. Suzuki,⁸ O. Tajima,⁸ F. Takasaki,⁸ K. Tamai,⁸ N. Tamura,²⁸ M. Tanaka,⁸ Y. Teramoto,²⁹ X. C. Tian,³² T. Tsuboyama,⁸ T. Tsukamoto,⁸ S. Uehara,⁸ T. Uglov,¹² K. Ueno,²⁵ S. Uno,⁸ P. Urquijo,²⁰ G. Varner,⁷ K. E. Varvell,³⁷ S. Villa,¹⁷ C. H. Wang,²⁴ M.-Z. Wang,²⁵ Q. L. Xie,¹⁰ B. D. Yabsley,⁴⁷ A. Yamaguchi,⁴¹ H. Yamamoto,⁴¹ Y. Yamashita,²⁷ M. Yamauchi,⁸ Heyoung Yang,³⁵ C. C. Zhang,¹⁰ J. Zhang,⁸ L. M. Zhang,³⁴ Z. P. Zhang,³⁴ V. Zhilich,¹ and D. Žontar^{18,13}

(The Belle Collaboration)

¹*Budker Institute of Nuclear Physics, Novosibirsk*

²*Chiba University, Chiba*

³*Chonnam National University, Kwangju*

⁴*University of Cincinnati, Cincinnati, Ohio 45221*

⁵*University of Frankfurt, Frankfurt*

⁶*Gyeongsang National University, Chinju*

⁷*University of Hawaii, Honolulu, Hawaii 96822*

⁸*High Energy Accelerator Research Organization (KEK), Tsukuba*

⁹*Hiroshima Institute of Technology, Hiroshima*

¹⁰*Institute of High Energy Physics, Chinese Academy of Sciences, Beijing*

¹¹*Institute of High Energy Physics, Vienna*

¹²*Institute for Theoretical and Experimental Physics, Moscow*

¹³*J. Stefan Institute, Ljubljana*

¹⁴*Kanagawa University, Yokohama*

¹⁵*Korea University, Seoul*

¹⁶*Kyungpook National University, Taegu*

¹⁷*Swiss Federal Institute of Technology of Lausanne, EPFL, Lausanne*

¹⁸*University of Ljubljana, Ljubljana*

¹⁹*University of Maribor, Maribor*

²⁰*University of Melbourne, Victoria*

²¹*Nagoya University, Nagoya*

²²*Nara Women's University, Nara*

²³*National Central University, Chung-li*

²⁴*National United University, Miao Li*

²⁵*Department of Physics, National Taiwan University, Taipei*

²⁶*H. Niewodniczanski Institute of Nuclear Physics, Krakow*

²⁷*Nihon Dental College, Niigata*

²⁸*Niigata University, Niigata*

²⁹*Osaka City University, Osaka*

³⁰*Osaka University, Osaka*

³¹*Panjab University, Chandigarh*

³²*Peking University, Beijing*

³³*Princeton University, Princeton, New Jersey 08544*

³⁴*University of Science and Technology of China, Hefei*

³⁵Seoul National University, Seoul

³⁶Sungkyunkwan University, Suwon

³⁷University of Sydney, Sydney NSW

³⁸Tata Institute of Fundamental Research, Bombay

³⁹Toho University, Funabashi

⁴⁰Tohoku Gakuin University, Tagajo

⁴¹Tohoku University, Sendai

⁴²Department of Physics, University of Tokyo, Tokyo

⁴³Tokyo Institute of Technology, Tokyo

⁴⁴Tokyo Metropolitan University, Tokyo

⁴⁵Tokyo University of Agriculture and Technology, Tokyo

⁴⁶University of Tsukuba, Tsukuba

⁴⁷Virginia Polytechnic Institute and State University, Blacksburg, Virginia 24061

⁴⁸Yonsei University, Seoul

Using a sample of 152 million $B\bar{B}$ pairs accumulated with the Belle detector at the KEKB e^+e^- collider, we perform a Dalitz plot analysis of the three-body charmed decay $B^- \rightarrow \Lambda_c^+ \bar{p} \pi^-$. The intermediate two-body decay $B^- \rightarrow \Sigma_c(2455)^0 \bar{p}$ is observed for the first time with a branching fraction of $(3.67_{-0.66}^{+0.74} \pm 0.36 \pm 0.95) \times 10^{-5}$ and a statistical significance of 8.4σ . We also observe a low-mass enhancement in the $(\Lambda_c^+ \bar{p})$ system, which can be parameterized as a Breit-Wigner with a mass of $(3.35_{-0.02}^{+0.01} \pm 0.02)$ GeV/ c^2 and a width of $(0.07_{-0.03}^{+0.04} \pm 0.04)$ GeV/ c^2 . We measure the product of the corresponding decay branching fractions to be $(3.87_{-0.72}^{+0.77} \pm 0.43 \pm 1.01) \times 10^{-5}$ with a statistical significance of 6.2σ . The errors are statistical, systematic, and that of the $\Lambda_c^+ \rightarrow pK^- \pi^+$ decay branching fraction.

PACS numbers: 13.25.Hw, 14.20.Lq

Recently three-body baryon production in charmless B decays has been studied with the Belle detector [1, 2, 3, 4]. Analysis of these decays shows a common feature: the invariant mass of the baryon-antibaryon system is peaked near threshold. This feature has generated much theoretical discussion and may be due to a fragmentation effect, production of resonances near threshold or final state interaction of the produced baryon-antibaryon system [5, 6, 7, 8, 9]. It is of interest to learn whether similar behavior is also observed in B decays to charmed baryons. The three-body decay $B^- \rightarrow \Lambda_c^+ \bar{p} \pi^-$ has been previously studied at CLEO [10] and Belle [11] with 9.2 fb^{-1} and 29.1 fb^{-1} of data, respectively. Evidence for $\Sigma_c(2455/2520)^0 \bar{p}$ intermediate states was obtained with limited statistics. Here we report on a Dalitz plot analysis of $B^- \rightarrow \Lambda_c^+ \bar{p} \pi^-$ decay based on a data sample of 140 fb^{-1} corresponding to $(152.0 \pm 0.7) \times 10^6$ $B\bar{B}$ pairs, accumulated at the $\Upsilon(4S)$ resonance with the Belle detector at the KEKB e^+e^- collider [12].

The Belle detector is a large-solid-angle magnetic spectrometer that consists of a three-layer silicon vertex detector (SVD), a 50-layer cylindrical drift chamber (CDC), a mosaic of aerogel threshold Čerenkov counters (ACC), a barrel-like array of time-of-flight scintillation counters (TOF), and an array of CsI(Tl) crystals (ECL) located inside a superconducting solenoidal coil that provides a 1.5 T magnetic field. An iron flux return located outside the coil is instrumented to detect muons and K_L^0 mesons (KLM). The detector is described in detail elsewhere [13]. We use a GEANT based Monte Carlo (MC) simulation to model the response of the detector and determine its

acceptance [14].

We detect the Λ_c^+ via the $\Lambda_c^+ \rightarrow pK^- \pi^+$, $p\bar{K}^0$, $\Lambda\pi^+$, $p\bar{K}^0\pi^+\pi^-$ and $\Lambda\pi^+\pi^+\pi^-$ decay channels. Inclusion of charge conjugate states is implicit unless otherwise stated. Neutral kaons are reconstructed in the $K_S^0 \rightarrow \pi^+\pi^-$ decay. Candidate Λ baryons are reconstructed in the decay $\Lambda \rightarrow p\pi^-$. The $B^- \rightarrow \Lambda_c^+ \bar{p} \pi^-$ events are identified by their energy difference $\Delta E = (\sum E_i) - E_{\text{beam}}$, and the beam-energy constrained mass $M_{\text{bc}} = \sqrt{E_{\text{beam}}^2 - (\sum \vec{p}_i)^2}$, where E_{beam} is the beam energy, and \vec{p}_i and E_i are the three-momenta and energies of the B meson decay products, all defined in the center-of-mass system of the e^+e^- collision. To suppress continuum background, we impose requirements on the angle between the thrust axis of the B candidate tracks and that of the other tracks and on the ratio of the second to the zeroth Fox-Wolfram moments [15]. Fig. 1 shows the

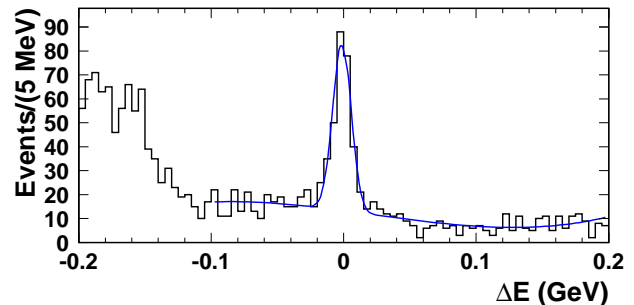


FIG. 1: ΔE distribution for $B^- \rightarrow \Lambda_c^+ \bar{p} \pi^-$ candidates. The curve shows the result of the fit.

ΔE distribution for $M_{\text{bc}} > 5.27$ GeV/ c^2 for the selected

B candidates. The signal yield is extracted by a fit to signal and background components. The signal shape is taken from MC while a third order polynomial is used to parameterize the background. This background shape is determined from a MC study that indicates a broad background below the signal due to continuum events and combinatorial backgrounds from other B decay modes, such as $\bar{B}^0 \rightarrow \Lambda_c^+ \bar{p} \pi^0$. We obtain 264 ± 20 signal events with a statistical significance of 17.1σ . The significance is calculated as $\sqrt{-2 \ln(\mathcal{L}_0/\mathcal{L}_{\max})}$, where \mathcal{L}_{\max} and \mathcal{L}_0 denote the maximum likelihoods with the fitted signal yield and with the yield fixed at zero, respectively.

Signals from two-body $B^- \rightarrow \Sigma_c(2455/2520)^0 \bar{p}$ intermediate decays, evidence for which has been obtained earlier [10, 11], are expected in the $M(\Lambda_c^+ \pi^-)$ distribution. Fig. 2(a) shows the $M(\Lambda_c^+ \pi^-)$ distribution around

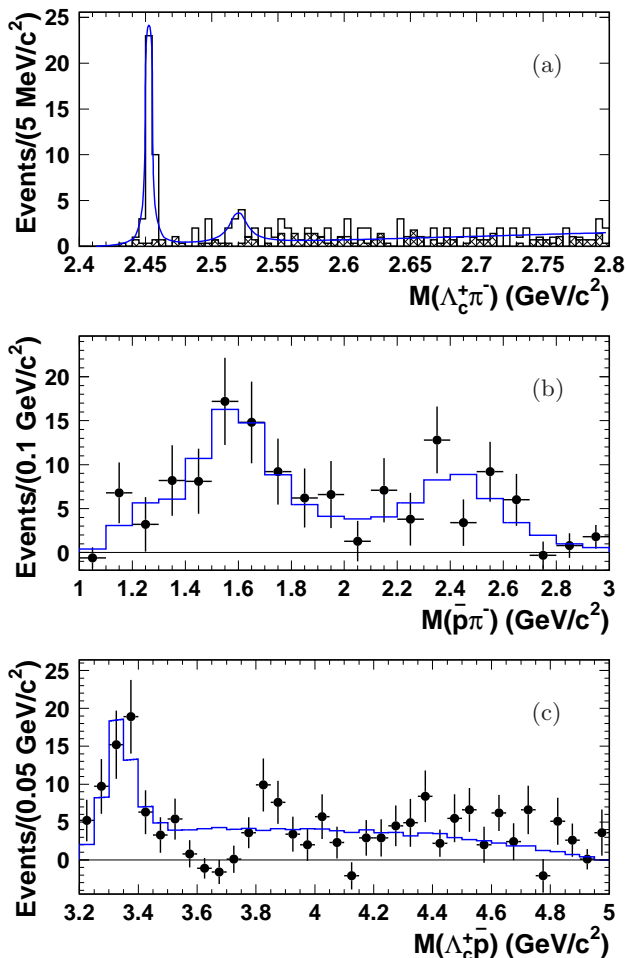


FIG. 2: (a) $M(\Lambda_c^+ \pi^-)$ distribution for the B signal region (open histogram) and fit results (curve); the distribution in the sidebands is also shown (hatched). (b,c) B^- yields (points) from fits to ΔE distributions, (b) in bins of $M(\bar{p}\pi^-)$, requiring $M(\Lambda_c^+ \pi^-) > 2.6 \text{ GeV}/c^2$ and $M(\Lambda_c^+ \bar{p}) > 3.5 \text{ GeV}/c^2$; and (c) in bins of $M(\Lambda_c^+ \bar{p})$, requiring $M(\Lambda_c^+ \pi^-) > 2.6 \text{ GeV}/c^2$ and $M(\bar{p}\pi^-) > 1.6 \text{ GeV}/c^2$. The histograms show fit results, see the text.

the $\Sigma_c(2455/2520)^0$ resonances for $B^- \rightarrow \Lambda_c^+ \bar{p} \pi^-$ decay

candidate events. The open histogram is the distribution from the B signal region ($|\Delta E| < 0.03 \text{ GeV}$ and $M_{bc} > 5.27 \text{ GeV}/c^2$). The hatched histogram is the distribution from sideband regions ($-0.10 \text{ GeV} < \Delta E < -0.04 \text{ GeV}$ or $0.04 \text{ GeV} < \Delta E < 0.20 \text{ GeV}$) normalized to the B signal region area. The curve shows the result of the fit, which includes the contribution from $\Sigma_c(2455/2520)^0 \rightarrow \Lambda_c^+ \pi^-$ decays and the background parameterized with a linear function. The $\Sigma_c(2455/2520)^0$ signal shapes are fixed from MC assuming a Breit-Wigner function convolved with the resolution function and using $\Sigma_c(2455/2520)^0$ masses and widths from Ref. [16]. To extract the yields for $B^- \rightarrow \Sigma_c(2455/2520)^0 \bar{p}$ decays, background from continuum and/or other B decays is taken into account by fitting simultaneously the B signal and sideband regions in the ΔE distribution. From the fit, we obtain $35.3^{+6.4}_{-6.0}$ signal events with a statistical significance of 8.2σ for the $B^- \rightarrow \Sigma_c(2455)^0 \bar{p}$ decay, and $12.6^{+5.4}_{-4.7}$ signal events with a statistical significance of 3.0σ for the $B^- \rightarrow \Sigma_c(2520)^0 \bar{p}$ decay.

Fig. 2(b) shows the $M(\bar{p}\pi^-)$ distribution for the $B^- \rightarrow \Lambda_c^+ \bar{p} \pi^-$ candidate events from fits to the ΔE distribution in 100 MeV bins of $(\bar{p}\pi^-)$ mass with constraints of $M(\Lambda_c^+ \pi^-) > 2.6 \text{ GeV}/c^2$ to remove Σ_c^0 intermediate states and $M(\Lambda_c^+ \bar{p}) > 3.5 \text{ GeV}/c^2$ to remove an enhancement at low $(\Lambda_c^+ \bar{p})$, which is discussed below. The histogram shows the result of a fit including the following contributions: three-body phase space, $B^- \rightarrow \Lambda_c^+ \bar{\Delta}(1232)^{--}$ decay as suggested by theory [17], and two other contributions, with parameters close to the $\Delta(1600)$ and $\Delta(2420)$ resonances tentatively referred to as $\Delta_X(1600)$ and $\Delta_X(2420)$. The signal shapes are fixed from the MC. Both three-body phase space and $\Delta(1232)$ contributions have a 0.5σ significance. The statistical significance of the $\Delta_X(1600)$ contribution is 6.7σ with a yield of 82 ± 12 events while that of the $\Delta_X(2420)$ is 4.7σ with a yield of 41 ± 9 events.

Fig. 2(c) shows the $M(\Lambda_c^+ \bar{p})$ distribution for $B^- \rightarrow \Lambda_c^+ \bar{p} \pi^-$ decay candidate events from fits to the ΔE distribution in 50 MeV bins of $(\Lambda_c^+ \bar{p})$ mass with $M(\Lambda_c^+ \pi^-) > 2.6 \text{ GeV}/c^2$ to remove Σ_c contributions and $M(\bar{p}\pi^-) > 1.6 \text{ GeV}/c^2$ to remove low $(\bar{p}\pi^-)$ masses. A low mass enhancement is observed. The histogram is the result of a fit parameterizing the distribution with a Breit-Wigner peak and feed-downs from the $B^- \rightarrow \Lambda_c^+ \bar{\Delta}_X(1600/2420)^{--}$ contributions. This fit gives a mass of $(3.35^{+0.01}_{-0.02}) \text{ GeV}/c^2$ and full width of $(0.07^{+0.04}_{-0.03}) \text{ GeV}/c^2$. The fit yield is 50 ± 10 events with a statistical significance of 5.6σ .

A second peak near $3.8 \text{ GeV}/c^2$ has a mass of $(3.84 \pm 0.01) \text{ GeV}/c^2$ and width of $(0.03 \pm 0.03) \text{ GeV}/c^2$. The yield of this peak is 15 ± 6 events and its statistical significance is only 2.8σ , so it was not studied any further.

To estimate systematic uncertainties of the mass and width of the peak at $3.35 \text{ GeV}/c^2$, we have performed fits with different background parameteriza-

tions, which included the contributions of the $B^- \rightarrow \Lambda_c^+ \bar{\Delta}_X(1600/2420)^{--}$ feed-downs with a free number of events or a broad Breit-Wigner with and without the second peak at $3.8 \text{ GeV}/c^2$. The mass variation is less than $0.02 \text{ GeV}/c^2$, and the width varies by less than $0.04 \text{ GeV}/c^2$.

We investigated the helicity distribution of the $(\Lambda_c^+ \bar{p})$ structure. The helicity angle, $\Theta(\Lambda_c^+ \bar{p})$, is defined as the angle between the Λ_c^+ momentum and the direction opposite to the B meson momentum in the $(\Lambda_c^+ \bar{p})$ rest frame. This distribution could distinguish between two possible interpretations of the $(\Lambda_c^+ \bar{p})$ low mass enhancement. If it is due to fragmentation, the distribution will be asymmetric, while for a resonance it will be symmetric [8]. In the case of a resonance, analysis of this distribution could provide information on the spin of the $(\Lambda_c^+ \bar{p})$ state. Fig. 3 shows the efficiency corrected helicity distribution for this

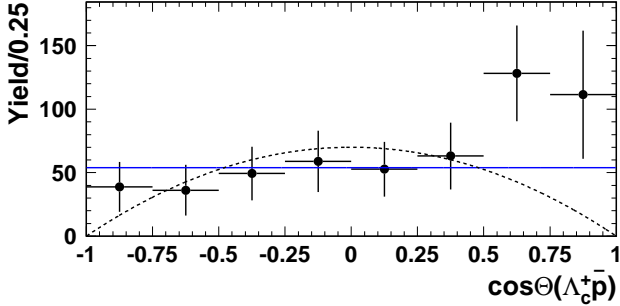


FIG. 3: The efficiency corrected helicity distribution for the $(\Lambda_c^+ \bar{p})$ structure. The solid line is the expectation for a $J = 0$ state, while the dashed line corresponds to $J = 1$.

decay for events from the region $M(\Lambda_c^+ \bar{p}) < 3.6 \text{ GeV}/c^2$, where the data points were obtained from fits to the ΔE distributions. The solid line is the result of the fit to the $J = 0$ hypothesis while the dashed one corresponds to the $J = 1$ case. The $J = 0$ hypothesis is slightly favored ($\chi^2/\text{ndf} = 0.97$) over the $J = 1$ case ($\chi^2/\text{ndf} = 1.58$). The observed helicity asymmetry is $\frac{|N_+ - N_-|}{N_+ + N_-} = 0.32 \pm 0.14$, where N_+ and N_- are the efficiency corrected numbers of events with $\cos \Theta(\Lambda_c^+ \bar{p}) > 0$ and < 0 , respectively. No definite conclusions can be drawn from the helicity studies with the statistics of this data sample.

We extract the contributions of intermediate states by a Dalitz plot analysis taking into account differences of the detection efficiencies for various intermediate states. The Dalitz plot of $M(\bar{p}\pi^-)^2$ vs $M(\Lambda_c^+ \pi^-)^2$ is shown in Fig. 4. It is subdivided into six regions suggested by the six states observed in two particle mass spectra:

- 1 $B^- \rightarrow \Sigma_c(2455)^0 \bar{p}$ $M(\Lambda_c^+ \pi^-) < 2.48 \text{ GeV}/c^2$;
- 2 $B^- \rightarrow \Sigma_c(2520)^0 \bar{p}$ $M(\Lambda_c^+ \pi^-) > 2.48 \text{ GeV}/c^2$,
- 3 $B^- \rightarrow \Lambda_c^+ \bar{\Delta}(1232)^{--}$ $M(\Lambda_c^+ \pi^-) < 2.6 \text{ GeV}/c^2$,
- 4 $B^- \rightarrow \Lambda_c^+ \bar{\Delta}_X(1600)^{--}$ $M(\Lambda_c^+ \pi^-) > 2.6 \text{ GeV}/c^2$,
- 5 $B^- \rightarrow \Lambda_c^+ \bar{\Delta}_X(2420)^{--}$ $M(\Lambda_c^+ \pi^-) > 2.6 \text{ GeV}/c^2$,
- 6 $(\Lambda_c^+ \bar{p})$ enhancement $M(\Lambda_c^+ \pi^-) > 2.0 \text{ GeV}/c^2$,

- $M(\bar{p}\pi^-) > 1.4 \text{ GeV}/c^2$,
- $M(\bar{p}\pi^-) < 2.0 \text{ GeV}/c^2$;
- $M(\Lambda_c^+ \pi^-) > 2.6 \text{ GeV}/c^2$,
- $M(\bar{p}\pi^-) > 2.0 \text{ GeV}/c^2$,
- $M(\Lambda_c^+ \bar{p}) > 3.6 \text{ GeV}/c^2$;
- $M(\Lambda_c^+ \bar{p}) > 2.0 \text{ GeV}/c^2$,
- $M(\Lambda_c^+ \bar{p}) < 3.6 \text{ GeV}/c^2$.

The $\Sigma_c(2455)^0$, $\Sigma_c(2520)^0$, $\bar{\Delta}(1232)^{--}$, $\bar{\Delta}_X(1600)^{--}$ and $\bar{\Delta}_X(2420)^{--}$ parameters are taken from [16]. The low mass $(\Lambda_c^+ \bar{p})$ enhancement is represented as a Breit-Wigner with mass $3.35 \text{ GeV}/c^2$ and full width $0.07 \text{ GeV}/c^2$ as indicated by the above analysis of the $(\Lambda_c^+ \bar{p})$. It is visible as a band in region 6 of Fig. 4. The B signal yield in the i -th region is $X_i = \sum_{j=1}^6 \varepsilon_{ij} \cdot Y_j$, where the probability ε_{ij} for the j -th intermediate state to be in the i -th region is taken from the signal MC, and six yields Y_j for each intermediate state are extracted from a simultaneous fit to six ΔE distributions.

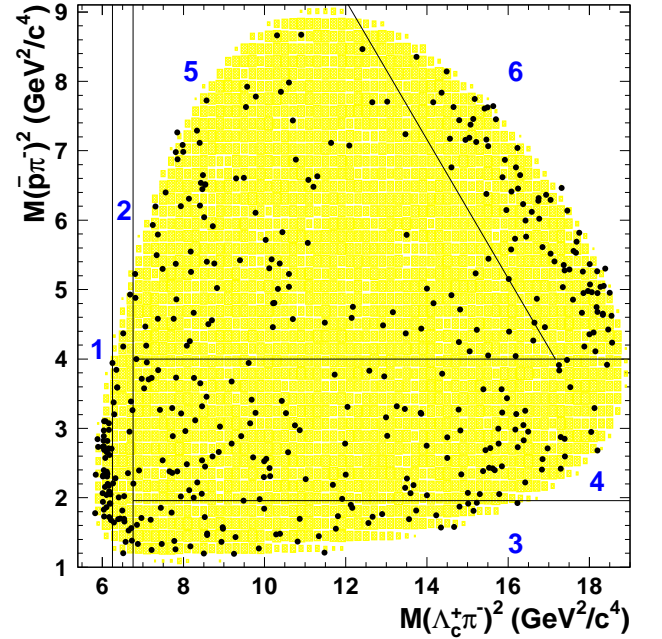


FIG. 4: The $M(\bar{p}\pi^-)^2$ vs $M(\Lambda_c^+ \pi^-)^2$ Dalitz plot subdivided into six regions.

The branching fraction \mathcal{B}_k for the k -th Λ_c^+ decay mode is calculated as $\mathcal{B}_k = N_k / (N_{B\bar{B}} \times \varepsilon_k \times \mathcal{B}_k(\Lambda_c^+))$, where N_k is the B signal yield. The detection efficiencies, ε_k , are determined from MC. The Λ_c^+ decay branching fractions $\mathcal{B}_k(\Lambda_c^+)$ are converted to the product $\mathcal{B}(\Lambda_c^+ \rightarrow pK^-\pi^+) \times \Gamma_k(\Lambda_c^+) / \Gamma(\Lambda_c^+ \rightarrow pK^-\pi^+)$ to remove the common uncertainty from $\mathcal{B}(\Lambda_c^+ \rightarrow pK^-\pi^+)$. The detection efficiency for the total signal yield N is $\varepsilon = \sum \varepsilon_k \times \Gamma_k(\Lambda_c^+) / \Gamma(\Lambda_c^+ \rightarrow pK^-\pi^+)$ and the overall branching fraction is $\mathcal{B} = N / (N_{B\bar{B}} \times \varepsilon \times \mathcal{B}(\Lambda_c^+ \rightarrow pK^-\pi^+))$. The fractions of charged and neutral B mesons are assumed to be equal.

The resulting yields, branching fractions and signifi-

cances for each intermediate state are listed in Table I. For the branching fractions, the first error is statistical and the second is systematic, whereas the third (26%) comes from the uncertainty in $\mathcal{B}(\Lambda_c^+ \rightarrow pK^- \pi^+)$.

Systematic uncertainties in the detection efficiencies arise from the track reconstruction efficiency (5–7% depending on the process, assuming a correlated systematic error of about 1% per charged track); the PID efficiency (about 7% assuming a correlated systematic error of 2% per proton and 1% per pion or kaon); and MC statistics (1–2%). The other uncertainties are associated with $\Gamma(\Lambda_c^+)/\Gamma(\Lambda_c^+ \rightarrow pK^- \pi^+)$ (1–2%); the number of $N_{B\bar{B}}$ events (0.5%); and the parameters of the low mass ($\Lambda_c^+ \bar{p}$) enhancement that can contribute up to 6% to the uncertainty of its branching fraction (but nothing to the uncertainty of the branching fractions of the other intermediate states). The total systematic error is estimated to be 9–11% depending on the intermediate state.

In summary, using a sample of 152 million $B\bar{B}$ pairs, accumulated with the Belle detector at the KEKB collider, we performed a Dalitz plot analysis of the three-body charmed decay $B^- \rightarrow \Lambda_c^+ \bar{p} \pi^-$. We report first observation of the two-body decay mode $B^- \rightarrow \Sigma_c(2455)^0 \bar{p}$ and measure its branching fraction to be $(3.67_{-0.66}^{+0.74} \pm 0.36 \pm 0.95) \times 10^{-5}$ with a statistical significance of 8.4σ . The branching fraction for $B^- \rightarrow \Sigma_c(2455)^0 \bar{p}$ is comparable to that for the only other known two-body baryonic decay $\bar{B}^0 \rightarrow \Lambda_c^+ \bar{p}$, which was discussed in an earlier publication [18]. We also observe a low mass enhancement in the $(\Lambda_c^+ \bar{p})$ system, which can be parameterized as a Breit-Wigner with a mass of $(3.35_{-0.02}^{+0.01} \pm 0.02)$ GeV/ c^2 and a width of $(0.07_{-0.03}^{+0.04} \pm 0.04)$ GeV/ c^2 . We measure the branching fraction of the B^- decay to this structure followed by its decay to $\Lambda_c^+ \bar{p}$ to be $(3.87_{-0.72}^{+0.77} \pm 0.43 \pm 1.01) \times 10^{-5}$ with a statistical significance of 6.2σ . The current data are not sufficient to determine whether this enhancement is a resonance, an effect due to fragmentation or a final state interaction of the produced baryon-antibaryon system. The total three-body $B^- \rightarrow \Lambda_c^+ \bar{p} \pi^-$ decay branching fraction has been measured to be $(20.1 \pm 1.5 \pm 2.0 \pm 5.2) \times 10^{-5}$, which is consistent with previous results [10, 11]. The branching fractions measurements supersede those in Ref. [11].

We thank the KEKB group for the excellent operation of the accelerator, the KEK cryogenics group for the efficient operation of the solenoid, and the KEK computer

group and the NII for valuable computing and SuperSINET network support. We acknowledge support from MEXT and JSPS (Japan); ARC and DEST (Australia); NSFC (contract No. 10175071, China); DST (India); the BK21 program of MOEHRD and the CHEP SRC program of KOSEF (Korea); KBN (contract No. 2P03B 01324, Poland); MIST (Russia); MHEST (Slovenia); SNSF (Switzerland); NSC and MOE (Taiwan); and DOE (USA).

* on leave from Nova Gorica Polytechnic, Nova Gorica

- [1] K. Abe *et al.* (Belle Collaboration), Phys. Rev. Lett. **88**, 181803 (2002).
- [2] K. Abe *et al.* (Belle Collaboration), Phys. Rev. Lett. **89**, 151802 (2002).
- [3] M.-Z. Wang *et al.* (Belle Collaboration), Phys. Rev. Lett. **90**, 201802 (2003).
- [4] M.-Z. Wang *et al.* (Belle Collaboration), Phys. Rev. Lett. **92**, 131801 (2004).
- [5] C.K. Chua, W.S. Hou and S.Y. Tsai, Phys. Rev. D **66**, 054004 (2002).
- [6] H.Y. Cheng and K.C. Yang, Phys. Rev. D **66**, 094009 (2002).
- [7] C.K. Chua and W.S. Hou, Eur. Phys. J. C **29**, 27 (2003).
- [8] J.L. Rosner, Phys. Rev. D **68**, 014004 (2003).
- [9] B. Kerbikov, A. Stavinsky, V. Fedotov, Phys. Rev. C **69**, 055205 (2004).
- [10] S.A. Dytman *et al.* (CLEO Collaboration), Phys. Rev. D **66**, 091101(R) (2002).
- [11] N. Gabyshev *et al.* (Belle Collaboration), Phys. Rev. D **66**, 091102(R) (2002).
- [12] S. Kurokawa and E. Kikutani, Nucl. Instrum. Meth., **A499**, 1 (2003), and other papers included in this Volume.
- [13] A. Abashian *et al.* (Belle Collaboration), Nucl. Instr. and Meth. A **479**, 117 (2002).
- [14] Events are generated with the CLEO group QQ program (<http://www.lns.cornell.edu/public/CLEO/soft/qq>). The detector response is simulated using GEANT: R. Brun *et al.*, GEANT 3.21, CERN Report DD/EE/84-1, 1984.
- [15] G.C. Fox and S. Wolfram, Phys. Rev. Lett. **41**, 1581 (1978).
- [16] S. Eidelman *et al.*, Phys. Lett. B **592**, 1 (2004).
- [17] H.Y. Cheng and K.C. Yang, Phys. Rev. D **67**, 034008 (2003).
- [18] N. Gabyshev *et al.* (Belle Collaboration), Phys. Rev. Lett. **90**, 121802 (2003).

TABLE I: Signal yields from the simultaneous fit, statistical significances, overall detection efficiencies (ϵ , see text) and branching fractions for intermediate decay modes in $B^- \rightarrow \Lambda_c^+ \bar{p} \pi^-$.

Mode	Signal yield, ev.	Signif., σ	Detection efficiency, %	Branching fraction \mathcal{B} , 10^{-5}
$B^- \rightarrow \Sigma_c(2455)^0 \bar{p}$	$32.6^{+6.6}_{-5.9}$	8.4	11.70	$3.67^{+0.74}_{-0.66} \pm 0.36 \pm 0.95$
$B^- \rightarrow \Sigma_c(2520)^0 \bar{p}$	$12.8^{+5.7}_{-5.0}$	2.9	13.36	$1.26^{+0.56}_{-0.49} \pm 0.12 \pm 0.33$ (< 2.7 90%CL)
$B^- \rightarrow \Lambda_c^+ \bar{\Delta}(1232)^{-}$	$8.9^{+7.6}_{-6.9}$	1.3	17.89	$0.65^{+0.56}_{-0.51} \pm 0.06 \pm 0.17$ (< 1.9 90%CL)
$B^- \rightarrow \Lambda_c^+ \bar{\Delta}_X(1600)^{-}$	$84.5^{+14.8}_{-13.8}$	7.5	18.85	$5.90^{+1.03}_{-0.96} \pm 0.55 \pm 1.53$
$B^- \rightarrow \Lambda_c^+ \bar{\Delta}_X(2420)^{-}$	$68.2^{+14.5}_{-13.4}$	6.1	19.08	$4.70^{+1.00}_{-0.92} \pm 0.43 \pm 1.22$
$(\Lambda_c^+ \bar{p})$ structure	$55.0^{+10.9}_{-10.2}$	6.2	18.69	$3.87^{+0.77}_{-0.72} \pm 0.43 \pm 1.01$
$B^- \rightarrow \Lambda_c^+ \bar{p} \pi^-$	262 ± 20	18.1		$20.1 \pm 1.5 \pm 2.0 \pm 5.2$